Journal of the Technical University of Gabrovo

https://mc04.manuscriptcentral.com/jtug

MATHEMATICAL MODELING OF DYNAMIC PROCESSES OF THE TERRESTRIAL ROBOTIC COMPLEX MANIPULATOR

Serhii Strutynskyi*, Roman Semenchuk

Igor Sikorsky Kyiv Polytechnic Institute

ARTICLE INFO

Article history:
Received 28 September 2020
Accepted 2 December 2020

Keywords:
robotic complexes, manipulators, mathematical modeling, dynamic processes, damping devices

ABSTRACT

The calculation scheme, that allow to investigate dynamic processes of the manipulator of the terrestrial robotic complex is offered. The dependences describing dynamics of the manipulator are received. A dynamic model of the manipulator has been developed. This model takes into account the possibility of using controlled damping devices. The obtained results take into account the influence of variable external factors on the dynamic processes of the ground-based robotic complex. The mathematical model of the manipulator can be combined with the existing mathematical model of the chassis. The proposed mathematical model has practical value and can be used in the development of a mechatronic system for stabilizing the position of the manipulator of the terrestrial robotic complex.

INTRODUCTION

Ground-based robotic systems are designed to solve a number of problems, in particular to perform special operations in difficult road conditions. They can move at high speeds on uneven ground. A typical design of a ground-based robotic complex includes a manipulator consisting of rods of constant length connected by rotary units. Effective performance of special operations by means of the robotic complex is possible on condition of maintenance of high dynamic characteristics. A promising solution to this problem is the use of controlled damper devices in the manipulator. To build an effective control system, it is necessary to develop a dynamic model of the manipulator, which involves the use of controlled damping devices.

EXPOSITION

In the scientific work [1] the nature of dynamic loads acting on a mobile robotic complex is determined. In separate works the research of drives of ground robotic complexes [2], in particular drives of manipulators [3] is given.

The rotary units of the manipulators are high-tech elements of the system and include an electric motor, a reducer and a bearing unit. Technical parameters of rotary units significantly affect the kinematic and dynamic characteristics of the manipulator. To some extent, the characteristics of the manipulator are determined by the deformation of the bars of constant length, due to the action of significant loads.

This paper uses the concept of "deformation" movement of the manipulator. This concept implies small deviations of the manipulator levers from their nominal position [4].

Consider a typical manipulator in a terrestrial robotic complex with six degrees of freedom. One of the most ergonomic designs of the ground-based robotic complex contains two rods of considerable length and six rotary units that provide the appropriate number of degrees of freedom. When studying the working processes of the manipulator, taking into account the peculiarities of its design, we can consider a simplified problem, ie to reduce this mechanism to a scheme that includes two levers and three kinematic pairs that connect these links. With such a scheme, you can immediately proceed to the consideration of a flat problem.

According to the proposed calculation scheme, the deviation of the levers of this manipulator leads to the movement of the hinges B and C of the manipulator of a typical design relative to the base of the ground robotic complex, including the hinge A (fig. 1).

Dynamic movements of the manipulator occur due to the movement of the chassis, which leads to vertical movements z_A of the hinge A of the manipulator and its transverse-angular movements at an angle θ. The manipulator is presented in the form of two masses m_B and m_C, which are concentrated in the hinges B and C. The levers of the manipulator are deformed, and the hinges of the rotary units correspond to their characteristic stiffness and coefficients of resistance. Controlled damping devices are installed in the hinge units, which create pulsed

* Corresponding author. E-mail: jswitch@ukr.net

dynamic loads R_1 and R_2, which are oriented at angles φ_1, φ_2 to the axes of the levers.

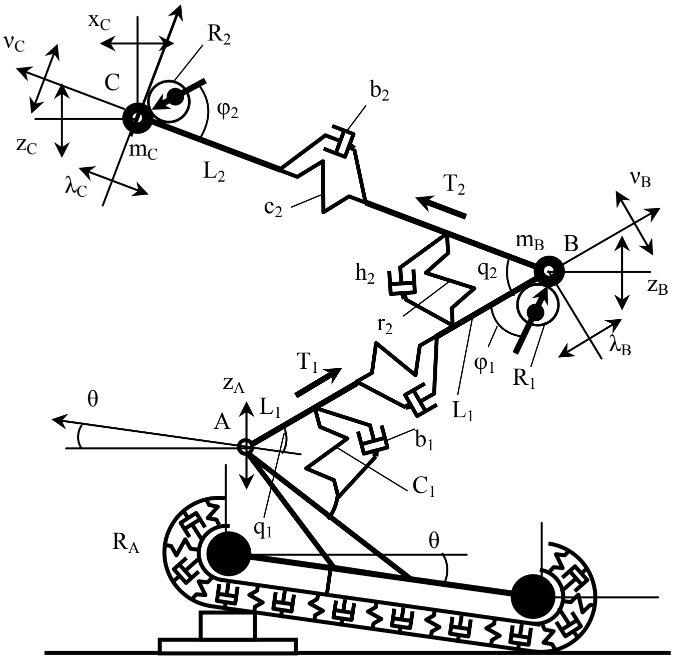

Fig. 1. Dynamic model of "deformation" movement of the manipulator

Let's make the equation of dynamic equilibrium of mass in the form of the sum of projections of forces on an axis of the lever of BC:

$$m_c \cdot \frac{d^2\lambda_c}{dt^2} = T_2 + R_2.cos\phi_2 ,$$

where m_c - the equivalent mass of the manipulator, optical devices and damper is concentrated at point C; λ_c - moving the mass m_c in the direction of the axis of the lever BC; T_2 - force at the intersection of the lever; R_2 - dynamic force action of the damper located at the end of the lever BC; ϕ_2 - the angle between the axis of the lever BC and the direction of action of the force R_2.

Transform this differential equation according to Laplace:

$$m_c S^2 \lambda_c = T_2 + R_2 \cos\phi_2 , \tag{1}$$

where S - Laplace operator; Λ_c - Laplace displacement image λ_c; R_2 and $R_2 \cos\phi_2$ - Laplace image of the force in the lever and the projection of the dynamic action of the damper on the axis of the lever BC.

From (1) we find the connection:

$$T_2 = m_c S^2 \Lambda_c - R_2 \cos\phi_2 . \tag{2}$$

Effort in the intersection of the lever BC defined as:

$$T_2 = (\lambda_B . \cos q_2 - \lambda_c) c_2 + \left(\frac{d\lambda_B}{dt} \cos q_2 - \frac{d\lambda_c}{dt} \right) b_2 , \tag{3}$$

where λ_B - mass movement m_B in the direction of the axis of the lever AB; q_2 - the nominal value of the angle between the axes of the levers AB and BC; c_2, b_2 - equivalent stiffness and tensile strength of the lever BC.

Transform the equation (3) according to Laplace:

$$T_2 = \Lambda_B . cosq_2 (c_2 + b_2 S) - \Lambda_C (c_2 + b_2 S) . \tag{4}$$

Substitute the value of the force from (4) into the dependence (2), we obtain after the transformations:

$$\Lambda_C \cdot (m_c S^2 + b_2 S + c_2) = \Lambda_B cosq_2 (c_2 + b_2 S) + R_2 cos\phi_2 \tag{5}$$

From here we define Λ_B:

$$\Lambda_B = \Lambda_c \frac{(m_c S^2 + b_2 S + c_2)}{(c_2 + b_2 S) cosq_2} - \frac{R_2 cos\phi_2}{(c_2 + b_2 S) cosq_2} . \tag{6}$$

From equation (6) we determine:

$$\Lambda_c = \Lambda_B \frac{cosq_2 (c_2 + b_2 S)}{m_c S^2 + b_2 S + c_2} - \frac{R_2 cos\phi_2}{(m_c S^2 + b_2 S + c_2)} . \tag{7}$$

We give the dependence (7) in the form of a block diagram (fig. 2).

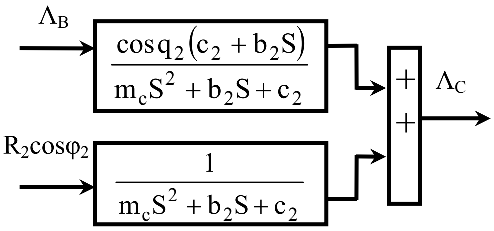

Fig. 2. Block diagram that establishes the relationship of longitudinal movements of the hinges B and C in the direction of the axes of the levers AB and BC

Add the sum of the moments of the forces acting on the lever BC relative to the point B:

$$m_c L_2^2 \frac{d^2 v_c}{dt^2} = M_2 \text{ - } R_2 L_2 sin\phi_2 , \tag{8}$$

where v_c - dynamic changes in the transverse angular position of the lever BC; M_2 - the moment of forces in the hinge with the drives located in a point B; L_2 - lever length BC.

Converted equation (8) according to Laplace:

$$m_c L_2^2 S^2 N_c = M_2 \text{ - } L_2 R_2 sin\phi_2 , \tag{9}$$

where N_c - Laplace transform of angular displacement v_2.

Moment of forces in the hinge B determined by the angular stiffness r_2 and the coefficient of resistance h_2 at transverse-angular movements of the lever BC relative to the lever AB.

The moment is described by dependence:

$$M_2 = (v_B - v_c) r_2 + \left(\frac{dv_B}{dt} - \frac{dv_c}{dt} \right) h_2 , \tag{10}$$

where v_B - dynamic changes in the transverse angular position of the lever AB.

Converted equation (10) according to Laplace:

$$M_2 = N_B [r_2 + h_2 S] - N_c [r_2 + h_2 S] , \tag{11}$$

where N_B - Laplace transform of angular displacement v_B.

Uniting the equation (9) and (11):

$$N_C (m_c L_2^2 S^2 + h_2 S + r_2) = N_B (r_2 + h_2 S) - L_2 R_2 \sin\phi_2 \tag{12}$$

From equation (12) we establish the dependences between the Laplace images of the angular displacements of the levers:

$$N_C = N_B \frac{(r_2 + h_2 S)}{(m_c L_2^2 S^2 + h_2 S + r_2)} - \frac{L_2 R_2 \sin\phi_2}{(m_c L_2^2 S^2 + h_2 S + r_2)} \quad (13)$$

$$N_B = N_C \frac{(m_c L_2^2 S^2 + h_2 S + r_2)}{r_2 + h_2 S} + \frac{L_2 R_2 \sin\phi_2}{r_2 + h_2 S} \quad (14)$$

Dependence (13) is given in the form of a block diagram (fig. 3).

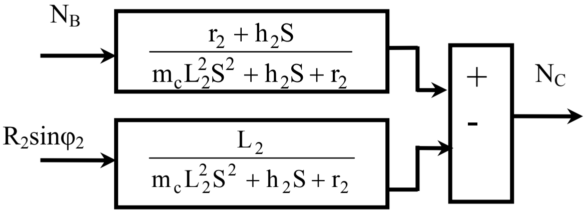

Fig. 3. Block diagram that establishes the relationship of transverse and angular movements of the levers: (moving the lever BC)

Defined the equation of dynamic equilibrium of equivalent mass m_B.

Composed the sum of the projections of the forces acting on the axis of the lever AB:

$$m_B \frac{d^2 \lambda_B}{dt^2} = T_1 + R_1 \cos\varphi_1 + T_2 \cos q_2 , \quad (15)$$

where T_1 - force at the intersection of the lever AB; R_1 - the dynamic action of the damper located at point B at the end of the lever AB; ϕ_1 - the angle between the axis of the lever AB and the direction of action of the force R_1.

Converted equation (15) according to Laplace:

$$m_B S^2 \Lambda_B = T_1 + T_2 \cos q_2 + R_1 \cos\phi_1 \quad (16)$$

The force at the intersection of the lever AB is determined by the formula:

$$T_1 = [z_A . \sin(q_1 - \theta) - \lambda_B] c_1 + \left[\frac{dz_A}{dt} \sin(q_1 - \theta) - \frac{d\lambda_B}{dt}\right] b_1 ,$$

where z_A - moving the hinge A; θ – chassis rotation angle; c_1, b_1 - equivalent stiffness and drag coefficient of the lever AB and the hinges A and B during tension-compression of the system in the direction of the axis of the lever AB; q_1 - nominal angular position of the hinge L_1 relative to the chassis.

Given that the transverse angular displacement of the chassis is negligible $q_1 << \theta$ we will receive:

$$T_1 = (z_A \sin q_1 - \lambda_B) c_1 + \left(\frac{dz_A}{dt} \sin q_1 - \frac{d\lambda_B}{dt}\right) b_1 \quad (17)$$

Converted equation (17) according to Laplace:

$$T_1 = Z_A \sin q_1 [c_1 + b_1 S] - \Lambda_B [c_1 + b_1 S], \quad (18)$$

where Z_A - Laplace image displacement z_A.

Let's substitute T_1 from (18) to (16), and T_2 from (2) in (16) and we will get:

$$\Lambda_B (m_B S^2 + b_1 S + c_1) = \cos q_2 . m_c S^2 \Lambda_c - \cos q_2 R_2 \cos\phi_2 + z_A \sin q_1 (c_1 + b_1 S) + R_1 \cos\phi_1 , \quad (19)$$

We give the dependence (19) in the form of a block diagram which is the output Λ_B (fig. 4).

From the condition of equality to zero of the sum of the moments of the forces acting on the lever AB relative to the point A we obtain the equation:

$$m_B . L_1^2 \frac{d^2 v_B}{dt^2} = M_1 - M_2 + R_1 L_1 \sin\phi_1 - T_2 L_1 \sin q_2 \quad (20)$$

where v_B - dynamic changes in the transverse angular position of the lever AB; M_1 - the moment of forces in the hinge with the drives located in point A; L_1 - lever length AB.

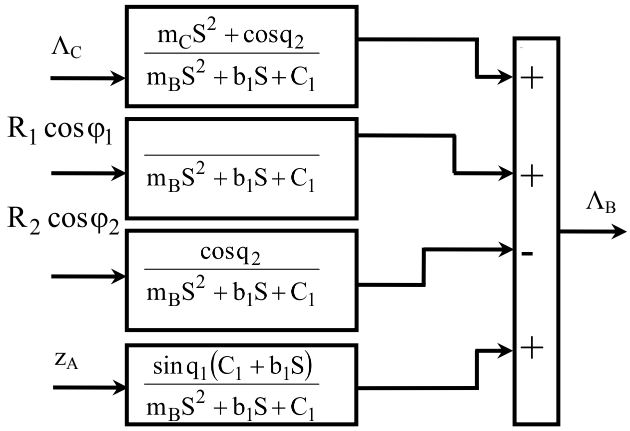

Fig. 4. Block diagram for determining the movement of the hinge B in the direction of the axis of the lever

Converted equation (20) according to Laplace:

$$m_B . L_1^2 S^2 . N_B = M_1 - M_2 + L_1 R_1 \sin\phi_1 - T_2 L_1 \sin q_2 \quad (21)$$

The moment of forces in the hinge A is determined by the angular stiffness of the hinge r_1 and the coefficient of resistance h_1 according to the dependence:

$$M_1 = (\theta - v_B) r_1 + \left(\frac{d\theta}{dt} - \frac{dv_B}{dt}\right) h_1 .$$

Let's transform this dependence on Laplace and we will receive:

$$M_1 = \theta (r_1 - h_1 S) - N_B (r_1 + h_1 S). \quad (22)$$

Substitute the value of the moment M_1 from dependence (22) в (21), the value of the moment M_2 from the formula (11) in (21), and the value of effort T_2 from the formula (2) in (21). We get after the transformations:

$$N_B (m_B L_1^2 S^2 + (h_1 + h_2) S + r_1 + r_2) = \theta (r_1 + h_1 S) + N_c (r_2 + h_2 S) - L_1 R_1 \sin\phi_1 - \sin q_2 m_c S^2 \Lambda_c - \sin q_2 R_2 \cos\phi_2 \quad (23)$$

We give this equality in the form of a block diagram (fig. 5).

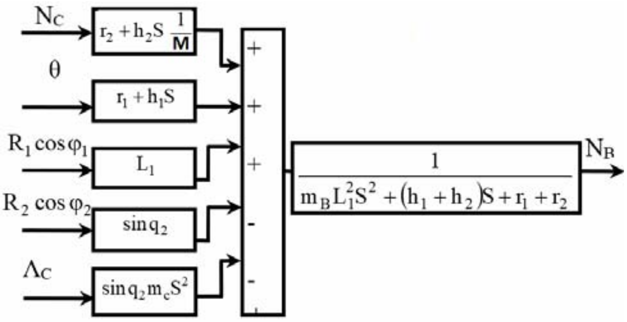

Fig. 5. The block diagram corresponds to the equilibrium conditions of the lever AB

The obtained equations and the corresponding block diagrams in closed form describe the dynamics of the elastic-dissipative system of the manipulator during its "deformation" motion. The inputs of the dynamic system of the manipulator are the vertical movement of the hinge A z_A and transverse-angular displacements of the chassis θ. Additional power inputs are the dynamic action of the dampers R_1 and R_2 and the angles of action of the forces created by the dampers ϕ_1 and ϕ_2.

The main output of the system is the vertical movement of the hinge C z_c, in which the optical device is installed. Additional outputs of the dynamic system of the manipulator are the force acting from the manipulator on the chassis (its vertical projection R_A) and the reaction moment of the hinge M_A.

Determine the movement of the hinges of the manipulator. Vertical movement of the hinge B will be:

$$z_B = \lambda_B \sin q_1 + L_1 v_B . \cos q_1 . \qquad (24)$$

The vertical movement of the hinge C will be:

$$z_c = z_B + \lambda_c \sin(q_2 - q_1) + L_2 v_c \cos(q_2 - q_1) . \qquad (25)$$

Uniting dependence (35) and (36) and a basic output models:

$$z_c = z_B \sin q_1 + v_B L_1 \cos q_1 + \lambda_c \sin(q_2 - q_1) + + v_c L_2 \cos(q_2 - q_1) . \qquad (26)$$

We transform this dependence according to Laplace and present it in the form of a block diagram (fig. 6).

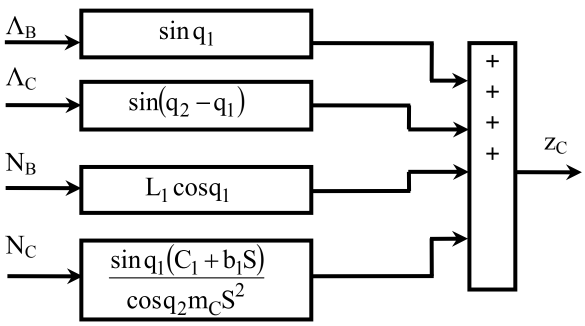

Fig. 6. Block diagram, which forms the total output of the system depending on the dynamic oscillations of the masses m_c and m_B

Determine the additional outputs of the dynamic system of the manipulator. The vertical force on the chassis in the area of the hinge A will be determined by:

$R_A = T_1 \sin q_1$.

Using dependence (18) we define the force R_A by the structural scheme (fig. 7a).

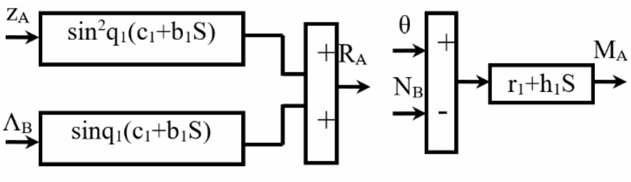

a b

Fig. 7. Block diagram for determining the force (a) and block diagram for determining the momentary load of the manipulator (b)

Load torque of the arm to the chassis in the hinge A will be: $M_A = M_1$.

Using dependence (22) we define the structural scheme of moment loading (fig. 7b).

Individual blocks-models are shown in fig. 2, 3, 4, 5, 6, 7a, 7b are combined into one model structure. Additional blocks are introduced into the model in which the projections of the forces of each damper on the axis of the lever and the perpendicular axis are calculated.

The stability of the computational procedure implemented in this model at different input parameters was checked. For this purpose transients at step change of position of the chassis are defined. From the analysis of the results of the calculation of transients it follows that the computational procedure works stably and the model can be used to calculate the parameters of the mechatronic control system of the damping devices of the manipulator of the ground robotic complex.

CONCLUSION

The proposed mathematical model of the "deformation" motion of the manipulator is characterized by the stability of the work and has its own outputs of movement of the hinge of the manipulator with optical devices installed on it. The manipulator model is combined with the existing mathematical model of the movement of the chassis with feedback and makes it possible to form the structure and select the parameters of the mechatronic system for stabilizing the position of the manipulator of the mobile ground-based robotic complex.

As a direction of further research, it is recommended to improve the control algorithm of the mechatronic system and experimental verification of the system of dynamic stabilization of the position of the optical devices of the mobile ground-based robotic complex.

REFERENCE

[1] Baoquan Li, Yongchun Fang, Guoqiang Hu, Xuebo Zhang. Model-Free Unified Tracking and Regulation Visual Servoing of Wheeled Mobile Robots. Journal Sensors and Actuators A: Physical, IEEE Transactions on Control Systems Technology, 24 (4) (2016) 1328–1339

[2] Voloshina A., Panchenko A., Panchenko I., Zasiadko A. Geometrical Parameters for Distribution Systems of Hydraulic Machines. Modern Development Paths of Agricultural Production. Springer, Cham (2019) 323-336

[3] Korayem M.H., Dehkordi S.F. Derivation of motion equation for mobile manipulator with viscoelastic links and revolute–prismatic flexible joints via recursive Gibbs–Appell formulations. Robotics and Autonomous Systems 103 (2018) 175-198

[4] Strutynskyi S. Defining the dynamic accuracy of positioning of spatial drive systems through consistent analysis of processes of different range of performance. Naukovyi Visnyk Natsionalnoho Hirnychoho Universytetu. Dnipro 3 (2018) 64–73